

1 **Moderate forest disturbance as a stringent test for gap and big-leaf models**

2

3 Ben Bond-Lamberty¹, Justin P. Fisk², Jennifer A. Holm³, Vanessa Bailey⁴, Gil Bohrer⁵,
4 and Christopher M. Gough⁶

5

6 1. Pacific Northwest National Laboratory, Joint Global Change Research Institute at the
7 University of Maryland–College Park, 5825 University Research Court, Suite 3500,
8 College Park, MD 20740, USA

9 2. Department of Geographical Sciences, 1150 LeFrak, University of Maryland
10 College Park, MD 20742, USA

11 3. Climate Sciences Department, Lawrence Berkeley National Laboratory, 1 Cyclotron
12 Rd., MS 74-0171, Berkeley, CA 94720, USA

13 4. Pacific Northwest National Laboratory, 902 Battelle Boulevard, Richland, WA 99352,
14 USA

15 5. Department of Civil, Environmental and Geodetic Engineering, The Ohio State
16 University, 470 Hitchcock Hall, 2070 Neil Avenue, Columbus, OH 43210, USA

17 6. Virginia Commonwealth University, Department of Biology, Box 842012, 1000 West
18 Cary Street, Richmond, Virginia 23284-2012 USA

19

20 Submitted to *Biogeosciences* special issue “Impacts of extreme climate events and
21 disturbances on carbon dynamics” June 27, 2014

22 Revised version submitted October 24, 2014

23 Revised version submitted December 10, 2014

24 **Abstract**

25 Disturbance-induced tree mortality is a key factor regulating the carbon balance
26 of a forest, but tree mortality and its subsequent effects are poorly represented processes
27 in terrestrial ecosystem models. It is thus unclear whether models can robustly simulate
28 moderate (non-catastrophic) disturbances, which tend to increase biological and structural
29 complexity and are increasingly common in aging U.S. forests. We tested whether three
30 forest ecosystem models—Biome-BGC, a classic big-leaf model, and the ZELIG and ED
31 gap-oriented models—could reproduce the resilience to moderate disturbance observed in
32 an experimentally manipulated forest (the Forest Accelerated Succession Experiment in
33 northern Michigan, USA, in which 38% of canopy dominants were stem girdled and
34 compared to control plots). Each model was parameterized, spun up, and disturbed
35 following similar protocols, and run for 5 years post-disturbance. The models replicated
36 observed declines in aboveground biomass well. Biome-BGC captured the timing and
37 rebound of observed leaf area index (LAI), while ZELIG and ED correctly estimated the
38 magnitude of LAI decline. None of the models fully captured the observed post-
39 disturbance C fluxes, in particular gross primary production or net primary production
40 (NPP). Biome-BGC NPP was correctly resilient, but for the wrong reasons, and could not
41 match the absolute observational values. ZELIG and ED, in contrast, exhibited large,
42 unobserved drops in NPP and net ecosystem production. The biological mechanisms
43 proposed to explain the observed rapid resilience of the C cycle are typically not
44 incorporated by these or other models. It is thus an open question whether most
45 ecosystem models will simulate correctly the gradual and less extensive tree mortality
46 characteristic of moderate disturbances.

47

48 **Introduction**

49 Natural and anthropogenic disturbances have numerous effects on the carbon (C)
50 and energy dynamics in forested ecosystems, and result in a variety of feedbacks between
51 terrestrial ecosystems and climate (Goetz et al., 2012). In particular, disturbance-induced
52 tree mortality is a key factor regulating the forest C balance, but a complicated one due to
53 high temporal and spatial heterogeneity (Vanderwel et al., 2013). Partly as a result,
54 mortality and disturbance are poorly represented processes in terrestrial ecosystem
55 models (Medvigy and Moorcroft, 2012; Peters et al., 2013; Dietze and Matthes, 2014).

56 Most North American forests are at some stage of recovery from either natural or
57 anthropogenic disturbance (Pan et al., 2011). In the U.S. upper Midwest and northeast,
58 low-severity disturbance is increasing in frequency and extent in regional forests, which
59 have regrown following stand-replacing disturbances over a century ago (Frelich and
60 Reich, 1995). The resulting cohort of fast-growing, deciduous trees is now past maturity
61 and beginning to decline, while longer-lived species representation is increasing (Gough
62 et al., 2010b). At the same time, forest disturbances in the region are transitioning away
63 from severe events that historically caused complete stand replacement, towards more
64 subtle disturbances that result in only partial canopy defoliation or loss of selected
65 species (Pregitzer and Euskirchen, 2004; Williams et al., 2012; Birdsey et al., 2006).
66 These subtler disturbances include partial harvests, wind, pathogenic insects, diseases,
67 and age-related senescence (e.g., Caspersen et al., 2000), which contribute to a gradient
68 of disturbance intensities across the landscape. Unlike stand-replacing disturbance,
69 moderate disturbances tend to increase biological and structural complexity, and

70 consequently are expected to have entirely different functional consequences for
71 ecosystems (Nave et al., 2011; Peters et al., 2013).

72 Moderate disturbances have mixed effects on successional trajectories of forest C
73 production and storage (Birdsey et al., 2006; Knohl et al., 2002; Vanderwel et al., 2013).
74 In many forests, C storage shows unexpected resilience or even resistance to partial
75 canopy defoliation (Hicke et al., 2011; Gough et al., 2013; Mathys et al., 2014) or
76 thinning (Granier et al., 2008). The reasons and mechanisms for different functional
77 responses to moderate disturbance are not clear, but these results have large potential
78 implications, as the long-assumed future decline of production in aging stands is expected
79 to reduce continental C sink strength (Birdsey et al., 2006). Recent empirical evidence
80 indicates however that net ecosystem production (NEP, the ecosystem carbon balance)
81 may be sustained or even increase in older forests that experience moderate disturbance
82 (Luyssaert et al., 2008). For example, NEP in the ~100-yr-old Harvard Forest has more
83 than doubled in the last 18 years (Keenan et al., 2012). More broadly, recent syntheses of
84 North America's mixed temperate forests found no evidence for a substantial decline in
85 NEP or net primary production (NPP) with age (He et al., 2012; Amiro et al., 2010).

86 Many ecosystem-scale models, designed for and tested in early- to mid-
87 successional forests with low biological and structural complexity, can be expected to
88 have trouble reproducing these results (Landsberg and Waring, 1997; Raulier, 1999; Law
89 et al., 2003; Li et al., 2003; Zhao et al., 2009). Such models are typically developed from,
90 and tested most thoroughly against, classic primary- and secondary-succession scenarios
91 featuring stand-replacing or at least gap-size disturbances (Peters et al., 2013; Weng et
92 al., 2012; Wang et al., 2014). Most model experiments using moderate (non-catastrophic)

93 disturbance intensities have been performed in the context of timber management, e.g.
94 assessing the sustainability of harvesting for a particular ecosystem or region (e.g., Peng
95 et al., 2002; Rolff and Ågren, 1999). As a result, it is unclear whether most ecosystem
96 models will be able to correctly simulate naturally occurring disturbances in mature
97 forests, which may be spatially more heterogeneous and generally do not involve biomass
98 removals. This is particularly important given the rapidly aging distribution of eastern
99 U.S. forests (USDA, 2013; Radeloff et al., 2012).

100 With moderate disturbances increasing in aging North American forests, and only
101 an emerging understanding of the mechanisms underpinning such forests' resilience to
102 disturbance, it is clearly important to understand how, and how well, forest models
103 simulate these events. Doing so not only provides a quantitative assessment of model
104 performance, but also may help identify knowledge gaps and processes missing or not
105 properly implemented in ecosystem models more generally. This study tested three forest
106 ecosystem models—a classic big-leaf model and two gap models—to understand how
107 well they reproduce observed resilience to moderate disturbance in an experimentally
108 manipulated forest, and explore specific mechanisms limiting model skill.

109

110 **Methods**

111 *Site description*

112 The study site is the University of Michigan Biological Station (UMBS, 45° 35.5'
113 N, 84° 43' W), nested within a secondary successional forest that is comprised of bigtooth
114 aspen (*Populus grandidentata*), northern red oak (*Quercus rubra*), red maple (*Acer*
115 *rubrum*), paper birch (*Betula papyrifera*), and eastern white pine (*Pinus strobus*).

116 Average overstory tree age in 2013 was 95 years. NEP in the unmanipulated footprint of
117 the UMBS control tower (US-UMBS) was 0.80-1.98 Mg C ha⁻¹ yr⁻¹ from 1999 to 2006,
118 averaging 1.58 Mg C ha⁻¹ yr⁻¹ with substantial landscape variation (Gough et al., 2009).
119 The forest was heavily logged in the late 1800s and early 1900s, and disturbed by fire
120 until 1923; its present-day plant composition is typical of many forests in the upper Great
121 Lakes region (Gough et al., 2007).

122

123 *The Forest Accelerated Succession Experiment*

124 The Forest Accelerated Succession Experiment (FASET) is an ongoing
125 experiment in which >6,700 aspen and birch trees (equivalent to 38% of stand basal area)
126 were stem girdled in 2008 within a 39 ha area. FASET is investigating how C storage and
127 fluxes change following moderate disturbance as Great Lakes forests transition from an
128 assemblage of early successional canopy trees to later successional canopy dominants.
129 The experiment's overarching hypothesis is that forest NEP will be resilient following
130 partial canopy defoliation and subsequently increase as canopies become more
131 biologically and structurally complex, and as nitrogen (N) not taken up by senescing
132 aspen and birch trees is redistributed to other, longer-lived species assuming canopy
133 dominance. The experiment employs a suite of paired C cycling measurements within
134 separate treatment and control meteorological flux tower footprints. The C cycling
135 parameters reported here for the control and treatment forests are aboveground biomass
136 (AGB), gross primary production (GPP), ecosystem respiration (ER), leaf area index
137 (LAI), total (above- and belowground) NPP, and NEP. Site methodological approaches
138 for the derivation of each are described by Gough et. al. (2013; 2008), but briefly, AGB

139 was estimated biometrically, using dendrometers and site-specific allometry; LAI from
140 litter traps; NPP from biometry and fine root cores; and ER, GPP, and NEP (here treated
141 as equivalent to net ecosystem exchange) from eddy covariance (Gough et al., 2013).

142 FASET results were most recently summarized by Gough et al. (2013). Briefly,
143 the girdling treatment successfully expedited mortality of early successional aspen and
144 birch, promoting an emerging canopy that approximates projected regional changes in
145 forest composition and structure (e.g., Wolter and White, 2002). In the first four years
146 following disturbance, GPP and ER both initially rose in the treatment plots relative to
147 the controls, while NPP and NEP were not significantly different in the control and
148 treatment forests even though LAI in the latter declined by up to 44% (summarized in
149 **Figure 1**). This high resilience of the C cycle was attributed to high N retention and rapid
150 reallocation of this limiting resource in support of new leaf area production as aspen and
151 birch declined (Nave et al., 2011). Decadal records of tree growth indicate that resilience
152 to age-related declines in NPP is highest where a diversity of canopy tree species is
153 present, because later successional species rapidly compensate for declining growth of
154 early successional species (Gough et al., 2010b). Investigators are also finding that
155 resilience of forest production to disturbance is dependent upon canopy structural
156 reorganizations that enhance C uptake by increasing light-use efficiency (Hardiman et al.,
157 2011; Gough et al., 2013), and by hydrodynamic responses that increase post-disturbance
158 water use efficiency in some species (Matheny et al., 2015).

159

160 *Model descriptions*

161 We tested three complementary models for their ability to replicate disturbance-
162 related changes in production and LAI observed in FASET; model attributes and
163 differences are summarized in **Table 1**. The first was a version of Biome-BGC (Running
164 and Hunt, 1993; Thornton et al., 2002). This model has coupled water, carbon, and
165 nitrogen cycles (Thornton and Zimmermann 2007), uses a Farquhar photosynthesis
166 submodel linked to prognostic leaf area, and runs on a daily timestep. The model
167 partitions NPP into the leaves, roots and stems using dynamic allocation patterns,
168 accounting for nitrogen and water limitations. It has been widely used for simulating
169 carbon flows in forest ecosystems (Kimball et al., 1997; Pietsch et al., 2003; Tatarinov
170 and Cienciala, 2009; Warren et al., 2011). We used a version of the model that
171 incorporates an explicit disturbance mechanism (Bond-Lamberty et al., 2007).

172 The second model tested was ZELIG, a gap model based on the original
173 principles of the JABOWA (Botkin et al., 1972) and FORET (Shugart and West, 1977)
174 models. ZELIG simulates the growth, death, and regeneration of individual trees (Urban,
175 1990; Urban et al., 1991) in a two-dimensional grid of 400 m² cells (i.e., gaps)
176 representing the forest canopy. Trees in each cell influence the availability of resources in
177 adjacent cells, although direct tree-to-tree interactions are not represented (Taylor et al.,
178 2009). ZELIG's main routines include growth, mortality, regeneration, and tracking
179 environmental conditions. In each model timestep, forest processes (e.g., seedling
180 establishment rate, diameter increment, survival rate) are reduced from their maximum
181 potential rates based on available resources. Potential tree regeneration, growth, and
182 survival are functions of light conditions, soil moisture, level of soil fertility resources,
183 and temperature. The model runs on a monthly timestep. Specific details on the

184 methodical approaches used in the model can be found in Urban et al. (1990; 1991) and
185 Larocque et al. (2006). ZELIG has been applied over many large-scale and diverse
186 landscapes (see list and further references in Holm et al., 2012).

187 The third model was ED, a terrestrial biosphere model that uses size- and age-
188 structure partial differential equations (PDEs) (Moorcroft et al., 2001) to approximate the
189 behavior of a stochastic gap model at medium to large scales. It combines an individual-
190 based gap model, describing a particular plant community, with biogeochemical
191 simulation of carbon, water, and nitrogen fluxes. Modeled processes include leaf-level
192 photosynthesis, explicit competition for water and mortality, and C and N allocation
193 above- and belowground (Moorcroft et al., 2001). Much of the soil model is based on that
194 of CENTURY (Parton et al., 1987). ED then models subgrid (~10 ha) disturbance
195 heterogeneity using its PDEs to approximate the behavior of a spatially distributed
196 ensemble of individual plants, and has been used for a variety of optimization and data
197 assimilation exercises (Medvigy et al., 2009).

198 It is important to note the complementary nature of these models: one is a classic
199 “big leaf” biogeochemical model focusing on process representation in a non-spatial
200 framework, another a gap model representative of its class, and the third emphasizes
201 mathematical scaling of a gap model across time and space. In addition, Biome-BGC’s
202 algorithms underlie the current version of the Community Land Model (CLM) (e.g.,
203 Bonan and Levis, 2010), while work is underway to make ED’s algorithms an optional
204 component in the next version of CLM. This provides a strong framework and motivation
205 for examining whether the high C cycling resilience observed following FASET’s
206 moderate disturbance can be reproduced in modeling experiments.

207

208 *Parameters and optimization*

209 Biome-BGC was subjected to a pre-experiment optimization exercise, with the
210 goal of algorithmically adjusting its parameters, within observational ranges, such that
211 model output best matched the pre-experiment carbon stocks and pools of the UMBS
212 forest. The choice of parameters to include was based on three factors: the known
213 sensitivities of Biome-BGC (White et al., 2000); our *a priori* knowledge of the FASET
214 research site and possible physiological mechanisms underlying forest resilience to
215 disturbance (Gough et al., 2013); and known uncertainties in measured data (C.M. Gough
216 et al., unpublished data). The final set of optimized parameters is shown in **Table 2**.
217 Constraining against observed C stocks can provide significant improvements in model
218 performance (Carvalhais et al., 2010); in this study, slow-turnover soil C, tree stem C,
219 and NPP were used as constraining variables. For the parameter-space search itself we
220 used a variant of the Simplex algorithm (Nelder and Mead, 1965) that uses a randomly
221 oriented set of basis vectors instead of fixed coordinate axes, as implemented
222 (*gsl_multimin_fminimizer_nmsimplex2rand*) in Gnu Scientific Library version GSL-1.16
223 (Gough, 2009). For each combination of parameter values selected by the algorithm,
224 Biome-BGC was ‘spun up’, i.e. its slow soil pools were brought to equilibrium, and the C
225 pools noted above compared to observed soil C values. A linear cost function ranked
226 model performance, imposing a large penalty if a parameter varied more than 2σ (based
227 on expert judgment) from its observed mean.

228 ZELIG was parameterized with species-specific and site-specific parameters
229 representative of the UMBS study site. The silvicultural and biological parameters for

230 each of the 8 temperate tree species required for ZELIG are listed in **Table 3**, with
231 species data collected in previous studies (Larocque et al., 2006; Leemans and Prentice,
232 1989; Holm et al., 2013). Soil field capacity (cm) and wilting point (cm) were determined
233 from measurements at the study site (unpublished data). We used allometric equations to
234 estimate aboveground biomass (AGB, Mg C ha⁻¹), which were generated from on-site
235 harvests at the UMBS site or from general allometric equations typical of northeastern
236 trees (Gough et al., 2008).

237 ED's parameters were used from the versions developed for studying both
238 anthropogenic and natural disturbance across U.S. forests (Hurtt et al., 2002; Fisk et al.,
239 2013). This configuration uses two tree functional types, a cold deciduous and an
240 evergreen. Allometric equations, leaf characteristics, and phenology parameters are
241 described in Hurtt et al. (2002) and summarized in **Table 4**.

242 For the main modeling experiment, Biome-BGC and ZELIG were driven by
243 identical reanalysis daily climate (NCEP, Kanamitsu et al., 2002), from 1970-2012 data
244 with mean values of air temperature (5.1 °C) and precipitation (575 mm yr⁻¹). In contrast,
245 ED used a climatology (i.e. with no year-to-year variation) comprised of the average
246 monthly diurnal cycle for light, temperature and humidity, and mean monthly
247 precipitation from the slightly warmer (mean 6.5 °C) North American Regional
248 Reanalysis for 1979-2010 (NARR, 2013). We recognize that using different climatic
249 inputs is not ideal, but Biome-BGC and ZELIG both took steps that made their results
250 comparable to those of ED. For Biome-BGC, we used ensembling (Thornton et al., 2002)
251 to characterize the mean climate and effect of interannual climate variability on model
252 outputs, reporting model outputs as means ± standard deviation computed by running the

253 model starting at each successive year in the climate data. For ZELIG, each year the
254 model stochastically generated new monthly temperature and precipitation, based on the
255 range provided by the NCEP data, thus also diminishing the effect of year-to-year
256 variability in the input data. In summary, all model results are reported based on mean
257 climatic conditions, not exact year-to-year changes.

258

259 *Modeling experiment*

260 As far as possible, we used the same experimental protocol with each of the three
261 models. The models were spun up, i.e. brought to a steady state with a mature forest, and
262 then the entire site was clear-cut, with all trees removed, i.e. harvested and the biomass
263 taken away. This approximates the known stand-replacing disturbances of the early 20th
264 century (Gough et al., 2007) in the UMBS forest. The models then allowed the forest to
265 recover over 90 years before imposing 13-14% harvests of basal area (ED and ZELIG)
266 and biomass (Biome-BGC) in 2008, 2009, and 2010. This approach was used, as opposed
267 to a single ~40% cut in 2008, to better mimic the slow death of girdled trees observed
268 over 2-3 years in the FASET study, as lagged mortality has been shown to exert strong
269 influence on modeling of forest disturbances (Dietze and Matthes, 2014). None of the
270 models allowed for tree girdling, and we used harvests as a second-best alternative; under
271 this protocol, the models remove tree stems while allowing leaves and fine litter to decay
272 on-site. This was consistent with our observations that girdled trees in FASET did not
273 senesce at once and remained standing for multiple years without significantly decaying
274 (Gough et al., 2013).

275 As ZELIG is an individual-based, species-specific forest demographic model, we
276 had the ability to more precisely replicate the FASET experiment by only harvesting
277 aspen and birch trees in the forest simulator. This allowed the remaining species to
278 continue growing, starting from their trajectories prior to the harvest but subject to less
279 competition due to the removal of aspen and birch trees. Prior to beginning the girdling
280 experiment, early-successional aspen and birch accounted for 49% of the basal area in
281 ZELIG (versus 38% in the FASET study site), and these species were preferentially
282 removed to match the 13-14% annual harvests used by the two other models. Although
283 ED also tracks the dynamics of individual trees, the configuration used here was limited
284 to two tree functional types (cf. **Table 4**). This precluded species specific girdling;
285 instead, 13-14% of the basal area across all individuals was harvested annually for the 3-
286 year period.

287 The disturbances occurred on May 1 in all models, replicating the timing of the
288 girdling treatment just prior to spring leaf-out (Gough et al., 2013). We examined six
289 primary model outputs at an annual resolution: GPP, ER, NPP, NEP (all these fluxes in
290 $\text{Mg C ha}^{-1} \text{ yr}^{-1}$), maximum LAI (unitless), and aboveground biomass (Mg C ha^{-1}),
291 comparing them to observed data for 0 to 4 years after disturbance. We particularly
292 focused on the models' structure and flux dynamics, i.e. whether they could replicate the
293 relative changes observed in FASET.

294

295 **Results**

296 Summarizing the models' absolute performance provides a useful context for
297 evaluating their relative changes discussed below. Pretreatment (i.e., control plots in

298 2007-8) aboveground biomass and LAI were $81.2 \pm 25.4 \text{ Mg C ha}^{-1}$ and 4.3 ± 1.3 ,
299 respectively (**Figure 1**). The models' comparable values ranged from 51 (Biome-BGC) to
300 101 (ED) to 109 (ZELIG) Mg C ha^{-1} , for biomass, and 1.5 to 4.9 to 6.4 for LAI,
301 respectively. Biome-BGC's forest, in other words, was significantly smaller than the
302 observed data; ZELIG's slightly larger; and that simulated by ED roughly comparable.
303 Observed pretreatment gross primary production (GPP) was $12.2 \text{ Mg C ha}^{-1} \text{ yr}^{-1}$, and
304 ecosystem respiration (ER) $9.1 \text{ Mg C ha}^{-1} \text{ yr}^{-1}$, resulting in net C fluxes of 6.6 and 2.2 $\text{Mg C ha}^{-1} \text{ yr}^{-1}$ for NPP and NEP, respectively (**Figure 1e,f**). The models' pretreatment GPP
305 values ranged from 2.2 (ED) to 6.8 (ZELIG) $\text{Mg C ha}^{-1} \text{ yr}^{-1}$, with Biome-BGC roughly
306 halfway between these two; all were thus much lower than observations. Control forest
307 NPP values of both Biome-BGC and ZELIG were low (2.6 and $3.7 \text{ Mg C ha}^{-1} \text{ yr}^{-1}$
308 respectively), while ED was $8.2 \text{ Mg C ha}^{-1} \text{ yr}^{-1}$. ZELIG was very close ($2.1 \text{ Mg C ha}^{-1} \text{ yr}^{-1}$
309 $^{-1}$) to the observed NEP value, with ED and Biome-BGC much smaller (1.4 and $0.3 \text{ Mg C ha}^{-1} \text{ yr}^{-1}$
310 $^{-1}$ respectively). In summary, pretreatment carbon stocks and fluxes varied
311 significantly among the models, with Biome-BGC consistently low—a smaller forest
312 producing and sequestering less C. The other two models varied in their fidelity to
313 observations, with only ED able to achieve observed NPP, while ZELIG was closest to
314 overall C balance, but neither could achieve the high observed GPP values.

316 Aboveground biomass declined by 35-36% between 2006 and 2010 in the FASET
317 experiment. The models tracked this well (**Figure 2a**), although the decline occurred
318 more slowly because of the protocol used in this modeling experiment (i.e., three
319 successive years of 13-14% cut instead of a single large girdling event). Leaf area index
320 was less well reproduced: ED and ZELIG came close to capturing the magnitude of the

321 observed decline (-30% and 33%, respectively, compared to -37 to -44% observed), but
322 not the observed rebound of LAI by 2011 (**Figure 2d**). Leaf area in Biome-BGC, in
323 contrast, captured the timing and rebound of observed LAI, but not its magnitude, as LAI
324 only declined by 13% in the model.

325 None of the models fully captured the main C flux dynamics observed in FASET.
326 GPP initially rose in the treatment plots relative to the observed plots, but the models all
327 simulated GPP declines (**Figure 1c**) of up to 5% (Biome-BGC), 10% (ED), and 14%
328 (ZELIG). The models also all produced modest ER declines for 2008-2010, whereas
329 observed ER rose by 10% relative to control values; this is perhaps not surprising, given
330 that our modeling protocol removed ‘girdled’ trees from the ecosystem. Observed net
331 primary production did not significantly differ between treatment and control plots
332 (**Figure 1f**), but the models all exhibited NPP declines, by up to 3% (Biome-BGC), 10%
333 (ED), and 14% (ZELIG). All models’ treatment NPP had, however, recovered to control
334 levels by 2012 (**Figure 2f**). Net ecosystem production was also unchanged in the
335 observations, while Biome-BGC NEP declined by 23-27% (**Figure 2e**). ED and ZELIG
336 recorded even larger drops, of 79% and 43% respectively, although NEP had, like NPP,
337 recovered to control levels four year following disturbance in all models.

338 The models’ skill—i.e., how well they replicated both the magnitude and timing of
339 all observed variables—is summarized in **Figure 3**, a Taylor plot (Taylor, 2001) that is
340 useful for summarizing both multiple aspects of complex models and relative skill. Here,
341 all models exhibited low correlation (0.08-0.29) with observations, high root-mean-
342 square difference (9-18%) between simulated and observed values, and high standard
343 deviation, implying overall low model skill.

344 In ZELIG, aspen and birch exhibited low to moderate resilience (i.e. full recovery
345 to pretreatment basal area was not achieved) following moderate forest disturbance. The
346 model also predicted which species thrived or declined post-disturbance (**Figure 4**). Of
347 the two treatment species that were girdled, aspen showed a stronger resilience and
348 recovered to 71% of pretreatment basal area after four years, increasing by $3.1 \text{ m}^2 \text{ ha}^{-1}$. In
349 contrast, birch remained at post-treatment basal area over the next 60 years, increasing by
350 only $0.2 \text{ m}^2 \text{ ha}^{-1}$. The ZELIG forest became dominated by red oak (**Figure 4**), with that
351 species' basal area increasing nearly two-fold, followed by sugar maple and white pine,
352 which increased by 72% and 6% respectively. Thirty years after disturbance, the total
353 basal area as predicted by ZELIG was 33.6 versus $32.7 \text{ m}^2 \text{ ha}^{-1}$ pretreatment, and
354 recovery of basal area (a proxy for recovery of biomass) was achieved, even though
355 ZELIG failed to capture the observed high resilience in C fluxes during the first four
356 years after disturbance.

357 Similarly, the reduction in number of individuals in ED resulted in a direct
358 reduction in LAI, due to the strict allometric relationships used. Because NPP and NEP
359 are so closely tied to LAI in ED, this resulted in low resistance to the disturbance event.
360

361 **Discussion**

362 Relatively few previous studies have examined how well models can simulate
363 non-catastrophic forest disturbance. Peters et al. (2013) used the PnET-CN model to
364 examine how disturbance type, intensity, and frequency influenced forest NPP for forest
365 stands across the upper Midwest, and found that increasing intensity had no effect for
366 deciduous species, but decreased evergreen NPP. Wang et al. (2014) also used PnET-CN

367 and reported that measured and modeled evergreen needleleaf forests had lower
368 resilience to disturbance than deciduous forests. This agrees with Biome-BGC's
369 behavior, in which broadleaf deciduous trees (such as simulated here) are less sensitive to
370 moderate disturbance than are evergreen conifers (Thornton et al., 2002). The interaction
371 of disturbance intensity and forest resilience thus has both short- and long-term effects,
372 presenting significant challenges to models (Seidl et al., 2014; Dietze and Matthes, 2014).

373

374 *Model mechanisms and behaviors*

375 Gough et al. (2013) proposed several mechanisms supporting sustained C uptake
376 and storage (in particular the fluxes NPP and NEP) after the FASET disturbance:
377 enhancement of canopy light use efficiency, maintenance of light absorption as later
378 successional species take advantage of increased light availability, and redistribution of N
379 from senescent to early successional trees (Nave et al., 2011). The three models used in
380 this study are highly variable in their assumptions, parameters, and processes, and it is
381 instructive to understand how and why each had difficulty reproducing the FASET results
382 with respect to these proposed mechanisms.

383 All the models here, along with most others (e.g. Potter et al., 2003), assume a
384 fixed light use efficiency (LUE): trees in the model can produce more or less leaf area,
385 intercepting more or less radiation, but that area will produce a fixed amount of
386 photosynthate under particular environmental conditions of light, temperature, etc. In
387 reality trees can produce leaves with different structural, chemical, and photosynthetic
388 characteristics (e.g., Sardans et al., 2012). These changes, integrated across leaves within
389 a forest canopy, would likely result in different post-disturbance biotic and abiotic

390 dynamics; FASET has already shown the assumption of a fixed LUE not to be true at the
391 stand level (Gough et al., 2013). Recent work has also shown that the use of a spatially-
392 variable LUE parameterization, using C flux measurements from the Fluxnet dataset, can
393 significantly improve the accuracy of modeled GPP (Madani et al., 2014).

394 Maintenance of canopy light absorption in the FASET forest depends on a
395 structurally heterogeneous canopy so that subdominant trees quickly increase their
396 absorption following the girdling of canopy dominants (Gough et al., 2013). We would
397 have expected, *a priori*, that ZELIG would be best able to simulate this dynamic, as it
398 models a wide range of competing tree species, both early and late-successional,
399 competing in the same forest (**Figure 4**). All models simulated small to moderate
400 declines in both GPP and ER with disturbance, in contrast to the small observational
401 increases. The differences were generally small, however, and both fluxes are not direct
402 observations, but rather derived from tower measurements of ecosystem exchange, and
403 thus less well constrained than NPP and NEP. For this reason we consider the models'
404 inability to replicate the *absolute* GPP and ER (which were two to three times higher than
405 simulations) more troubling than their failure to exactly match the relative patterns shown
406 in **Figure 2**. NPP and NEP are better constrained observationally than are derived fluxes.
407 Biome-BGC best maintained these fluxes with disturbance, but for the wrong reason: too-
408 resilient leaf area (**Figure 2b**), rather than by increasing LUE when LAI declined in the
409 FASET study. We note however that the Biome-BGC phenology submodel was quite
410 accurate (cf. Gough et al., 2010a), a critical first step to accurately simulate stand C
411 dynamics (Richardson et al., 2012).

412 The proximal reason for Biome-BGC's too-strong resilience is that the fraction of
413 photosynthetically active radiation absorbed by the canopy, FPAR, does not diminish
414 change linearly with LAI changes. Radiation transmission and absorption through
415 canopies is a complex, computationally expensive process, and the three models studied
416 here all use a common simplification: Beer's law (Campbell and Norman, 1998), which
417 models it as an exponential decrease downwards through the canopy. Biome-BGC,
418 ZELIG, and ED also all assume a (mostly) equal extinction coefficient, and this implies
419 that the models' FPAR declines theoretically peaked at 3%, 12%, and 8%, respectively
420 (**Figure 5**), compared to 6% as measured in the field (Gough et al., 2013). The
421 mathematical form of Beer's law means that FPAR declines are smallest at low and high
422 LAI values. For Biome-BGC, with its low-biomass forest, this meant relatively small
423 FPAR declines with disturbance; small to moderate quantities of stored C and N lost to
424 disturbance; and enough stored C resources to fully leaf out the canopy and support
425 photosynthesis over the growing season.

426 ZELIG and ED both matched the observed LAI decline, and reasonably
427 approximated FPAR as well, but exhibited large declines in NPP and NEP for both
428 models. In ZELIG, even with the post-disturbance increase in available light, the
429 remaining subdominant species were not able to quickly increase their growth to make up
430 the difference in NPP loss. This may be due to the inherent growth and life history
431 strategies of these subdominant species, which is accounted for in the species
432 parameterization and initialization of ZELIG (**Table 3**). Only one species, red oak,
433 recovered quickly (**Figure 4**), while the remaining dominant species and subdominant
434 species could not contribute to an increase in NPP and NEP. Based on the current model

435 structure of ZELIG, leaf production and leaf loss are tightly linked with NPP and NEP;
436 therefore the decline in LAI corresponded to a resulting decline in C fluxes.

437 In a separate study, ZELIG-TROP, a modified version of ZELIG that simulates
438 tropical forests, was successful at replicating a non-significant change in NPP as a result
439 of gradual, less extensive tree mortality (Holm et al., 2014). That study used a continual
440 low-level elevated mortality rate as a treatment, i.e. doubling annual background
441 mortality rate, and ZELIG-TROP predicted highly resilient NPP. However, following a
442 one-time dramatic disturbance event (removing 20% of basal area) NPP also declined,
443 matching the modeled results seen here. Thus the ZELIG results are characteristic of the
444 model and not dependent on the particular forest type, soils, or climate of the FASET
445 experiment.

446 In ED, despite the increase in light availability following disturbance, the
447 remaining undisturbed trees were not able to respond sufficiently to offset NPP loss. This
448 may be in part to the limited number of plant functional types used here not representing
449 the competition of early and late successional species. Additionally, ED's scaling of
450 individual trees to stand dynamics does not maintain the full level of canopy complexity,
451 which may be required for resilience to a disturbance of this type.

452 Among the models tested here, nitrogen redistribution and limitation was only
453 possible in Biome-BGC, as ZELIG lacks an N cycle, and ED's integrated N cycle was
454 not parameterized or enabled in this study. Biome-BGC's integrated N cycle
455 encompasses N fixation, deposition, and leaching, plant growth, and microbial
456 decomposition, and should, in theory, constrain C uptake in many circumstances
457 (Thornton et al., 2007). Such an effect was not noticeable here, however, as equal

458 percentages of C and N were removed in the Biome-BGC disturbances (data not shown);
459 this implies leaching/loss, i.e. a lack of N conservation as opposed to what was observed
460 in FASET (Nave et al., 2011). This may also partly be an artifact, as all models used stem
461 biomass removals to simulate the real-world girdling (although in Biome-BGC leaves
462 were transferred to the litter pool, providing some N reallocation). We speculate,
463 however, that excessive N limitation was a factor in the model's inability to match the C
464 stock and flux values of the UMBS forest.

465 In summary, the biological mechanisms proposed (Gough et al., 2013) to explain
466 the carbon-cycle resilience of a mid-successional forest to disturbance are ones that most
467 models either do not simulate (integrated C and N cycles, changing light use efficiency)
468 or do so only crudely (canopy structure, heterotrophic respiration). At fine spatial scales,
469 factors such as canopy structure can be simulated, but the computational demands are
470 large and thus impractical for larger-scale models (Caspersen et al., 2011), consideration
471 that inspired the development of models such as ED (Moorcroft et al., 2001). Similarly,
472 how to translate the N-recycling microbial dynamics into ecosystem- to global-scale
473 models is an area of intense research (Wieder et al., 2013), as most models (including
474 those tested here) use a few conceptual soil pools following simple first-order kinetics. C-
475 N integration inside such models is increasingly common (Zaehle et al., 2014; Thornton
476 et al., 2007), enabling N redistribution and limitation dynamics, and should improve
477 future simulations of moderate disturbances.

478

479 **Conclusions**

480 The FASET results were unexpected and intriguing (Nave et al., 2011; Gough et
481 al., 2013; Hardiman et al., 2013). How well can current forest models simulate such
482 moderate, i.e. not stand-replacing, disturbances? Not all disturbances, even of the same
483 severity, equally affect biogeochemical processes that support recovery—for example,
484 slow versus immediate tree death have very different consequences (Franklin et al.,
485 1987). Our results suggest that **some** ecosystem models, developed to simulate processes
486 following stand-replacing disturbances, may not simulate gradual death scenarios well
487 (McDowell et al., 2013), specifically nonlinear or threshold responses of the carbon cycle
488 in disturbance intensity (Stuart-Haëntjens et al., 2014) over short timescales. Their skill
489 over longer (decadal) periods remains an open question. This is particularly important as
490 the moderate disturbances associated with slow tree death (insect outbreaks, fungal
491 pathogens) are on the rise worldwide (Allen et al., 2010) and in aging U.S. forests. It is
492 thus increasingly important to confront models with non-catastrophic disturbance
493 scenarios.

494

495 **Acknowledgements**

496 BBL and VLB were supported by the Office of Science of the U.S. Department of
497 Energy, as part of the Terrestrial Ecosystem Sciences Program. JAH was supported by
498 Jeffrey Chambers for part of this work. CMG and FASET were supported by the Climate
499 and Environmental Sciences Division, Office of Science, U.S. Department of Energy
500 (DOE) [Award No. DE-SC0006708], and by the Ameriflux Management Project [Flux
501 506 Core Site agreement No. 7096915] through Lawrence Berkeley National Laboratory.
502 We acknowledge the University of Michigan Biological Station for infrastructure and

503 logistics support, and are grateful for the insightful comments of two anonymous
504 referees.

505

506 **References**

- 507 Allen, C. D., Macalady, A. K., Chenchouni, H., Bachelet, D., McDowell, N. G.,
508 Vennetier, M., Kitzberger, T., Ringling, A., Breshears, D. D., Hogg, E. H.,
509 Gonzalez, P., Fensham, R., Zhang, Z., Castro, J., Demidova, N., Lim, J.-H.,
510 Allard, G., Running, S. W., Semerci, A., and Cobb, N.: A global overview of
511 drought and heat-induced tree mortality reveals emerging climate change risks for
512 forests, *Forest Ecol. Manage.*, 259, 660-684, [10.1016/j.foreco.2009.09.001](https://doi.org/10.1016/j.foreco.2009.09.001), 2010.
- 513 Amiro, B. D., Barr, A. G., Barr, J. G., Black, T. A., Bracho, R., Brown, M., Chen, J. M.,
514 Clark, K. L., Davis, K. J., Desai, A. R., Dore, S., Engel, V., Fuentes, J. D.,
515 Goldstein, A. H., Goulden, M. L., Kolb, T. E., Lavigne, M. B., Law, B. E.,
516 Margolis, H. A., Martin, T. A., McCaughey, J. H., Misson, L., Montes-Helu, M.
517 C., Noormets, A., Randerson, J. T., Starr, G., and Xiao, J.: Ecosystem carbon
518 dioxide fluxes after disturbance in forests of North America, *J. Geophys. Res.-*
519 *Biogeosci.*, 115, G00K02, [10.1029/2010JG001390](https://doi.org/10.1029/2010JG001390), 2010.
- 520 Birdsey, R. A., Pregitzer, K. S., and Lucier, A.: Forest carbon management in the United
521 States: 1600-2100, *Journal of Environmental Quality*, 35, 1461-1469,
522 [10.2134/jeq2005.0162](https://doi.org/10.2134/jeq2005.0162), 2006.
- 523 Bonan, G. B., and Levis, S.: Quantifying carbon-nitrogen feedbacks in the Community
524 Land Model (CLM4), *Geophys. Res. Lett.*, 37, L07401, [10.1029/2010GL042430](https://doi.org/10.1029/2010GL042430),
525 2010.

- 526 Bond-Lamberty, B., Peckham, S. D., Ahl, D. E., and Gower, S. T.: The dominance of fire
527 in determining carbon balance of the central Canadian boreal forest, *Nature*, 450,
528 89-92, [10.1038/nature06272](https://doi.org/10.1038/nature06272), 2007.
- 529 Botkin, D. B., Janak, J. F., and Wallis, J. R.: Rationale, limitations and assumptions of a
530 northeastern forest growth simulator, *IBM Journal of Research and Development*,
531 16, 101-116, 1972.
- 532 Campbell, G. S., and Norman, J. M.: *An Introduction to Environmental Biophysics*,
533 Springer-Verlag, New York, 286 pp., 1998.
- 534 Carvalhais, N., Reichstein, M., Ciais, P., Collatz, G. J., Mahecha, M. D., Montagnani, L.,
535 Papale, D., Rambal, S., and Seixas, J.: Identification of vegetation and soil carbon
536 pools out of equilibrium in a process model via eddy covariance and biometric
537 constraints, *Global Change Biol.*, 16, 2813-2829, [10.1111/j.1365-](https://doi.org/10.1111/j.1365-2486.2010.02173.x)
538 [2486.2010.02173.x](https://doi.org/10.1111/j.1365-2486.2010.02173.x), 2010.
- 539 Caspersen, J. P., Pacala, S. W., Jenkins, J. C., Hurtt, G. C., Moorcroft, P. R., and Birdsey,
540 R. A.: Contributions of land-use history to carbon accumulation in U.S. forests,
541 *Science*, 290, 1148-1151, [10.1126/science.290.5494.1148](https://doi.org/10.1126/science.290.5494.1148), 2000.
- 542 Caspersen, J. P., Vanderwel, M. C., Cole, W. G., and Purves, D.: How stand productivity
543 results from size- and competition-dependent growth and mortality, *PLOS ONE*,
544 6, e28660, [10.1371/journal.pone.0028660](https://doi.org/10.1371/journal.pone.0028660), 2011.
- 545 Dietze, M. C., and Matthes, J. H.: A general ecophysiological framework for modelling
546 the impact of pests and pathogens on forest ecosystems, *Ecology Letters*, 17,
547 1418-1426, [10.1111/ele.12345](https://doi.org/10.1111/ele.12345), 2014.
- 548 Fisk, J. P., Hurtt, G. C., Chambers, J. Q., Zeng, H., Dolan, K. A., and Negrón-Juárez, R.

- 549 I.: The impacts of tropical cyclones on the net carbon balance of eastern US
550 forests (1851–2000), *Environ. Res. Lett.*, 8, 045017, 10.1088/1748-
551 9326/8/4/045017, 2013.
- 552 Franklin, J. F., Shugart, H. H., and Harmon, M. E.: Tree death as an ecological process:
553 the causes, consequences and variability of tree mortality, *BioScience*, 37, 550-
554 556, 10.2307/1310665, 1987.
- 555 Frelich, L. E., and Reich, P. B.: Spatial patterns and succession in a Minnesota southern-
556 boreal forest, *Ecological Monographs*, 65, 325-346, 1995.
- 557 Goetz, S. J., Bond-Lamberty, B., Harmon, M. E., Hicke, J. A., Houghton, R. A.,
558 Kasischke, E. S., Law, B. E., McNulty, S. G., Meddens, A. J. H., Mildrexler, D.,
559 O'Halloran, T. L., and Pfeifer, E. M.: Observations and assessment of forest
560 carbon recovery following disturbance in North America, *J. Geophys. Res.-*
561 *Biogeosci.*, 117, G02022, 10.1029/2011JG001733, 2012.
- 562 Gough, C. M., Vogel, C. S., Kazanski, C., Nagel, L., Flower, C. E., and Curtis, P. S.:
563 Coarse woody debris and the carbon balance of a north temperate forest, *Forest*
564 *Ecol. Manage.*, 244, 60-67, 10.1016/j.foreco.2007.03.039, 2007.
- 565 Gough, C. M., Vogel, C. S., Schmid, H. P., and Curtis, P. S.: Multi-year convergence of
566 biometric and meteorological estimates of forest carbon storage, *Agric. Forest*
567 *Meteorol.*, 148, 158-170, 10.1016/j.agrformet.2007.08.004, 2008.
- 568 Gough, C. M., Flower, C. E., Vogel, C. S., Dragoni, D., and Curtis, P. S.: Whole-
569 ecosystem labile carbon production in a north temperate deciduous forest, *Agric.*
570 *Forest Meteorol.*, 149, 1531-1540, 10.1016/j.agrformet.2009.04.006, 2009.
- 571 Gough, C. M., Flower, C. E., Vogel, C. S., and Curtis, P. S.: Phenological and

- 572 Temperature Controls on the Temporal Non-Structural Carbohydrate Dynamics of
573 *Populus grandidentata* and *Quercus rubra*, *Forests*, 1, 65-81, 10.3390/f1010065,
574 2010a.
- 575 Gough, C. M., Vogel, C. S., Hardiman, B., and Curtis, P. S.: Wood net primary
576 production resilience in an unmanaged forest transitioning from early to middle
577 succession, *Forest Ecol. Manage.*, 260, 36-41, 10.1016/j.foreco.2010.03.027
578 2010b.
- 579 Gough, C. M., Hardiman, B., Nave, L. E., Bohrer, G., Maurer, K. D., Vogel, C. S.,
580 Nadelhoffer, K. J., and Curtis, P. S.: Sustained carbon uptake and storage
581 following moderate disturbance in a Great Lakes forest, *Ecol. Appl.*, 23, 1202-
582 1215, 10.1890/12-1554.1, 2013.
- 583 Granier, A., Breda, N., Longdoz, B., Gross, P., and Ngao, J.: Ten years of fluxes and
584 stand growth in a young beech forest at Hesse, north-eastern France, *Ann. For.*
585 *Sci.*, 65, art. no. 704, 10.1051/forest:2008052, 2008.
- 586 Hardiman, B., Bohrer, G., Gough, C. M., Vogel, C. S., and Curtis, P. S.: The role of
587 canopy structural complexity in wood net primary production of a maturing
588 northern deciduous forest *Ecology*, 92, 1818-1827, 10.1890/10-2192.1, 2011.
- 589 Hardiman, B., Gough, C. M., Halperin, A., Hofmeister, K. L., Nave, L. E., Bohrer, G.,
590 and Curtis, P. S.: Maintaining high rates of carbon storage in old forests: A
591 mechanism linking canopy structure to forest function, *Forest Ecol. Manage.*, 298,
592 111-119, 10.1016/j.foreco.2013.02.031, 2013.
- 593 He, L., Chen, J. M., Pan, Y., Birdsey, R. A., and Kattge, J.: Relationships between net
594 primary productivity and forest stand age in U.S. forests, *Glob. Biogeochem.*

- 595 Cycles, 26, GB3009, 10.1029/2010GB003942, 2012.
- 596 Hicke, J. A., Allen, C. D., Desai, A. R., Dietze, M. C., Hall, R. J., Hogg, E. H., Kashian,
597 D. M., Moore, D. J. P., Raffa, K. F., Sturrock, R. N., and Vogelmann, J. E.:
598 Effects of biotic disturbances on forest carbon cycling in the United States and
599 Canada, *Global Change Biol.*, 18, 7-34, 10.1111/j.1365-2486.2011.02543.x, 2011.
- 600 Holm, J. A., Shugart, H. H., Van Bloem, S. J., and Larocque, G. R.: Gap model
601 development, validation, and application to succession of secondary subtropical
602 dry forests of Puerto Rico, *Ecol. Model.*, 233, 70-82,
603 10.1016/j.ecolmodel.2012.03.014, 2012.
- 604 Holm, J. A., Thompson, J. R., McShea, W. J., and Bourg, N. A.: Interactive effects of
605 chronic deer browsing and canopy gap disturbance on forest successional
606 dynamics, *Ecosphere*, 4, art. 44, 10.1890/es13-00223.1, 2013.
- 607 Holm, J. A., Chambers, J. Q., Collins, W. D., and Higuchi, N.: Forest response to
608 increased disturbance in the Central Amazon and comparison to Western Amazon
609 forests, *Biogeosciences*, 11, 5773-5794, 10.5194/bg-11-5773-2014, 2014.
- 610 Hurtt, G. C., Pacala, S. W., Moorcroft, P. R., Caspersen, J. P., Shevliakova, E.,
611 Houghton, R. A., and Moore III, B.: Projecting the future of the U.S. carbon sink,
612 *Proc. Nat. Acad. Sci.*, 99, 1389-1394, 10.1073/pnas.012249999, 2002.
- 613 Kanamitsu, M., Ebisuzaki, W., Woollen, J., Yang, S.-K., Hnilo, J. J., Fiorino, M., and
614 Potter, G. L.: NCEP–DOE AMIP-II Reanalysis (R-2), *Bulletin of the American
615 Meteorological Society*, 83, 1631-1643, 10.1175/BAMS-83-11-1631, 2002.
- 616 Keenan, T. F., Davidson, E. A., Moffat, A. M., Munger, J. W., and Richardson, A. D.:
617 Using model-data fusion to interpret past trends, and quantify uncertainties in

- 618 future projections, of terrestrial ecosystem carbon cycling, *Global Change Biol.*,
619 18, 2555-2569, 10.1111/j.1365-2486.2012.02684.x, 2012.
- 620 Kimball, J. S., Thornton, P. E., White, M. A., and Running, S. W.: Simulating forest
621 productivity and surface-atmosphere carbon exchange in the BOREAS study
622 region, *Tree Physiol.*, 17, 589-599, 1997.
- 623 Knohl, A., Kolle, O., Minayeva, T. Y., Milyukova, I. M., Vygodskaya, N. N., Foken, T.,
624 and Schulze, E.-D.: Carbon dioxide exchange of a Russian boreal forest after
625 disturbance by wind throw, *Global Change Biol.*, 8, 231-246, 2002.
- 626 Landsberg, J. J., and Waring, R. H.: A generalised model of forest productivity using
627 simplified concepts of radiation-use efficiency, carbon balance and partitioning,
628 *Forest Ecol. Manage.*, 95, 209-228, 10.1016/S0378-1127(97)00026-1, 1997.
- 629 Larocque, G. R., Archambault, L., and Delisle, C.: Modelling forest succession in two
630 southeastern Canadian mixedwood ecosystem types using the ZELIG model,
631 *Ecol. Model.*, 199, 350-362, 10.1016/j.ecolmodel.2006.05.010, 2006.
- 632 Law, B. E., Sun, O. J., Campbell, J. S., Van Tuyl, S., and Thornton, P. E.: Changes in
633 carbon storage and fluxes in a chronosequence of ponderosa pine, *Global Change*
634 *Biol.*, 9, 510-524, 2003.
- 635 Leemans, R., and Prentice, I. C.: FORSKA: A general forest succession model,
636 *Meddelanden, Vaxtbiologiska institutionen, Uppsala, Sweden*, 2, 1-145, 1989.
- 637 Li, Z., Apps, M. J., Kurz, W. A., and Banfield, E.: Temporal changes of forest net
638 primary production and net ecosystem production in west central Canada
639 associated with natural and anthropogenic disturbances, *Can. J. For. Res.*, 33,
640 2340-2351, 10.1139/x03-168, 2003.

- 641 Luysaert, S., Schulze, E.-D., Börner, A., Knohl, A., Hessenmöller, D., Law, B. E., Ciais,
642 P., and Grace, J.: Old-growth forests as global carbon sinks, *Nature*, 455, 213-
643 215, 10.1038/nature07276, 2008.
- 644 Madani, N., Kimball, J. S., Affleck, D. L. R., Kattge, J., van Bodegom, P. M., Reich, P.
645 B., and Running, S. W.: Improving ecosystem productivity modeling through
646 spatially explicit estimation of optimal light use efficiency, *J. Geophys. Res.-*
647 *Biogeosci.*, 119, 1755-1769, 10.1002/2014JG002709, 2014.
- 648 Matheny, A. M., Bohrer, G., Vogel, C. S., Morin, T. H., He, L., Frasson, R. P. d. M.,
649 Mirfenderesgi, G., Schäfer, K. V. R., Gough, C. M., Ivanov, V. Y., and Curtis, P.
650 S.: Species-specific transpiration responses to intermediate disturbance in a
651 northern hardwood forest, *J. Geophys. Res.-Biogeosci.*, in press,
652 10.1002/2014JG002804, 2015.
- 653 Mathys, A., Black, T. A., Nesic, Z., Nishio, G., Brown, M., Spittlehouse, D. L., Fredeen,
654 A. L., Bowler, R., Jassal, R. S., Grant, N. J., Burton, P. J., Trofymow, J. A., and
655 Meyer, G.: Carbon balance of a partially harvested mixed conifer forest following
656 mountain pine beetle attack and its comparison to a clear-cut, *Biogeosciences*, 10,
657 5451-5463, 10.5194/bg-10-5451-2013, 2014.
- 658 McDowell, N. G., Fisher, R. A., Xu, C., Domec, J.-C., Höltta, T., Mackay, D. S., Sperry,
659 J. S., Boutz, A., Dickman, L. T., Gehres, N., Limousin, J. M., Macalady, A. K.,
660 Martínez-Vilalta, J., Mencuccini, M., Plaut, J. A., Ogée, J., Pangle, R. E., Rasse,
661 D. P., Ryan, M. G., Sevanto, S., Waring, R. H., Williams, A. P., Yopez, E. A., and
662 Pockman, W. T.: Evaluating theories of drought-induced vegetation mortality
663 using a multimodel–experiment framework, *New Phytol.*, 200, 304-321,

- 664 10.1111/nph.12465, 2013.
- 665 Medvigy, D., Wofsy, S. C., Munger, J. W., Hollinger, D. Y., and Moorcroft, P. R.:
- 666 Mechanistic scaling of ecosystem function and dynamics in space and time:
- 667 Ecosystem Demography model version 2, *J. Geophys. Res.-Biogeosci.*, 114,
- 668 G01002, 10.1029/2008JG000812, 2009.
- 669 Medvigy, D., and Moorcroft, P. R.: Predicting ecosystem dynamics at regional scales: an
- 670 evaluation of a terrestrial biosphere model for the forests of northeastern North
- 671 America, *Philosophical Transactions of the Royal Society of London Series B*,
- 672 367, 222-235, 10.1098/rstb.2011.0253, 2012.
- 673 Moorcroft, P. R., Hurtt, G. C., and Pacala, S. W.: A method for scaling vegetation
- 674 dynamics: the Ecosystem Demography model (ED), *Ecological Monographs*, 71,
- 675 557-586, 10.1890/0012-9615(2001)071[0557:AMFSVD]2.0.CO;2, 2001.
- 676 Nave, L. E., Gough, C. M., Maurer, K. D., Bohrer, G., Le Moine, J., Munoz, A. B.,
- 677 Nadelhoffer, K. J., Sparks, J. P., Strahm, B. D., Vogel, C. S., and Curtis, P. S.:
- 678 Disturbance and the resilience of coupled carbon and nitrogen cycling in a north
- 679 temperate forest, *J. Geophys. Res.-Biogeosci.*, 116, G04016,
- 680 10.1029/2011JG001758, 2011.
- 681 Nelder, J. A., and Mead, R.: A simplex method for function minimization, *Computer*
- 682 *Journal*, 7, 308-313, doi:10.1093/comjnl/7.4.308, 1965.
- 683 Pan, Y., Chen, J. M., Birdsey, R. A., McCullough, K., He, L., and Deng, F.: Age
- 684 structure and disturbance legacy of North American forests, *Biogeosciences*, 8,
- 685 715-732, 10.5194/bg-8-715-2011, 2011.
- 686 Parton, W. J., Schimel, D. S., Cole, C. V., and Ojima, D. S.: Analysis of factors

- 687 controlling soil organic matter levels in Great Plains grasslands, *Soil Science*
688 *Society of America Journal*, 51, 1173-1179, 1987.
- 689 Peng, C., Jiang, H., Apps, M. J., and Zhang, Y.: Effects of harvesting regimes on carbon
690 and nitrogen dynamics of boreal forests in central Canada: a process model
691 simulation, *Ecol. Model.*, 155, 177-189, 10.1016/S0304-3800(02)00134-5, 2002.
- 692 Peters, E. B., Wythers, K. R., Bradford, J. B., and Reich, P. B.: Influence of disturbance
693 on temperate forest productivity, *Ecosystems*, 16, 95-110, 10.1007/s10021-012-
694 9599-y, 2013.
- 695 Pietsch, S. A., Hasenauer, H., Kucera, J., and Cermák, J.: Modeling effects of
696 hydrological changes on the carbon and nitrogen balance of oaks in floodplains,
697 *Tree Physiol.*, 23, 735-746, 2003.
- 698 Potter, C. S., Klooster, S., Myneni, R. B., Genovese, V., Tan, P.-N., and Kumar, V.:
699 Continental-scale comparisons of terrestrial carbon sinks estimated from satellite
700 data and ecosystem modeling 1982-1998, *Global Planet. Change*, 39, 201-213,
701 2003.
- 702 Pregitzer, K. S., and Euskirchen, E. S.: Carbon cycling and storage in world forests:
703 biome patterns relating to forest age, *Global Change Biol.*, 10, 2052-2077,
704 10.1111/j.1365-2486.2004.00866.x, 2004.
- 705 Radeloff, V. C., Nelson, E., Plantinga, A. J., Lewis, D. J., Helmers, D., Lawler, J. J.,
706 Withey, J. C., Beaudry, F., Martinuzzi, S., Butsic, V., Lonsdorf, E., White, D. C.,
707 and Polasky, S.: Economic-based projections of future land use in the
708 conterminous United States under alternative policy scenarios, *Ecol. Appl.*, 22,
709 1036-1049, 2012.

- 710 Raulier, F.: Canopy photosynthesis of sugar maple (*Acer saccharum*): comparing big-leaf
711 and multilayer extrapolations of leaf-level measurements., *Tree Physiol.*, 19, 407-
712 420, 1999.
- 713 Richardson, A. D., Anderson, R. S., Arain, M. A., Barr, A. G., Bohrer, G., Chen, G.,
714 Chen, J. M., Ciais, P., Davis, K. J., Desai, A. R., Dietze, M. C., Dragoni, D.,
715 Garrity, S. R., Gough, C. M., Grant, R. F., Hollinger, D. Y., Margolis, H. A.,
716 McCaughey, J. H., Migliavacca, M., Monson, R. K., Munger, J. W., Poulter, B.,
717 Raczka, B. M., Ricciuto, D. M., Sahoo, A. K., Schaefer, K., Tian, H.-Q., Vargas,
718 R., Verbeeck, H., Xiao, J., and Xue, Y.: Terrestrial biosphere models need better
719 representation of vegetation phenology: results from the North American Carbon
720 Program Site Synthesis, *Global Change Biol.*, 18, 566-584, 10.1111/j.1365-
721 2486.2011.02562.x, 2012.
- 722 Rolff, C., and Ågren, G. I.: Predicting effects of different harvesting intensities with a
723 model of nitrogen limited forest growth, *Ecol. Model.*, 118, 193-211,
724 10.1016/S0304-3800(99)00043-5, 1999.
- 725 Running, S. W., and Hunt, R. E.: Generalization of a forest ecosystem process model for
726 other biomes, BIOME-BGC, and an application for global-scale models, in:
727 *Scaling Physiologic Processes: Leaf to Globe*, edited by: Ehleringer, J. R., and
728 Field, C. B., Academic Press, San Diego, CA, 141-158, 1993.
- 729 Sardans, J., Rivas-Ubach, A., and Peñuelas, J.: The C:N:P stoichiometry of organisms
730 and ecosystems in a changing world: A review and perspectives, *Perspectives in*
731 *Plant Ecology and Evolution*, 14, 33-47, 10.1016/j.ppees.2011.08.002, 2012.
- 732 Seidl, R., Rammer, W., and Spies, T. A.: Disturbance legacies increase the resilience of

- 733 forest ecosystem structure, composition, and functioning, *Ecol. Appl.*, 24, 2063-
734 2077, 10.1890/14-0255.1, 2014.
- 735 Shugart, H. H., and West, D. C.: Development of an Appalachian deciduous forest
736 succession model and its application to assessment of the impact of the chestnut
737 blight, *Journal of Environmental Management*, 5, 161-179, 1977.
- 738 Stuart-Haëntjens, E. J., Curtis, P. S., Fahey, R. T., Vogel, C. S., and Gough, C. M.: Forest
739 net primary production exhibits a threshold response to increasing disturbance
740 severity *Ecosystems*, submitted, 2014.
- 741 Tatarinov, F. A., and Cienciala, E.: Long-term simulation of the effect of climate changes
742 on the growth of main Central-European forest tree species, *Ecol. Model.*, 220,
743 3081-3088, 10.1016/j.ecolmodel.2009.01.029, 2009.
- 744 Taylor, A. R., Chen, H. Y. H., and VanDamme, L.: A review of forest succession models
745 and their suitability for forest management planning, *Forest Science*, 55, 23-36,
746 2009.
- 747 Taylor, K. E.: Summarizing multiple aspects of model performance in a single diagram,
748 *J. Geophys. Res.*, 106, 7183-7192, 2001.
- 749 Thornton, P. E., Law, B. E., Gholz, H. L., Clark, K. L., Falge, E., Ellsworth, D. S.,
750 Goldstein, A. H., Monson, R. K., Hollinger, D. Y., Falk, M., Chen, J., and Sparks,
751 J. P.: Modeling and measuring the effects of disturbance history and climate on
752 carbon and water budgets in evergreen needleleaf forests, *Agric. Forest Meteorol.*,
753 113, 185-222, [10.1016/S0168-1923\(02\)00108-9](https://doi.org/10.1016/S0168-1923(02)00108-9), 2002.
- 754 Thornton, P. E., Lamarque, J.-F., Rosenbloom, N. A., and Mahowald, N. M.: Influence of
755 carbon-nitrogen cycle coupling on land model response to CO₂ fertilization and

- 756 climate variability, *Glob. Biogeochem. Cycles*, 21, Art. No. GB4018,
757 10.1029/2006GB002868, 2007.
- 758 Urban, D. L.: A Versatile Model to Simulate Forest Pattern: A User's Guide to ZELIG
759 Version 1.0. , University of Virginia, Charlottesville, Virginia, 1990.
- 760 Urban, D. L., Bonan, G. B., Smith, T. M., and Shugart, H. H.: Spatial applications of gap
761 models, *Forest Ecol. Manage.*, 42, 95-110, 10.1016/0378-1127(91)90067-6, 1991.
- 762 Vanderwel, M. C., Coomes, D. A., and Purves, D.: Quantifying variation in forest
763 disturbance, and its effects on aboveground biomass dynamics, across the eastern
764 United States, *Global Change Biol.*, 19, 1504-1517, 10.1111/gcb.12152, 2013.
- 765 Wang, W., Xiao, J., Ollinger, S. V., Desai, A. R., Chen, J. M., and Noormets, A.:
766 Quantifying the effects of harvesting on carbon fluxes and stocks in northern
767 temperate forests, *Biogeosciences*, 11, 6667-6682, 10.5194/bg-11-6667-2014,
768 2014.
- 769 Warren, J. M., Pötzelsberger, E., Wullschleger, S. D., Thornton, P. E., Hasenauer, H., and
770 Norby, R. J.: Ecohydrologic impact of reduced stomatal conductance in forests
771 exposed to elevated CO₂, *Ecohydrology*, 4, 196-210, 10.1002/eco.173, 2011.
- 772 Weng, E., Luo, Y., Wang, W., Wang, H., Hayes, D. J., McGuire, A. D., Hastings, A., and
773 Schimel, D. S.: Ecosystem carbon storage capacity as affected by disturbance
774 regimes: A general theoretical model, *J. Geophys. Res.-Biogeosci.*, 117, G03014,
775 10.1029/2012JG002040, 2012.
- 776 White, M. A., Thornton, P. E., Running, S. W., and Nemani, R. R.: Parameterization and
777 sensitivity analysis of the BIOME-BGC terrestrial ecosystem model: net primary
778 production controls, *Earth Interact.*, 4, paper no. 3, 1-85, 2000.

- 779 Wieder, W. R., Bonan, G. B., and Allison, S. D.: Global soil carbon projections are
780 improved by modelling microbial processes, *Nature Climate Change*, 3, 909-912,
781 10.1038/NCLIMATE1951, 2013.
- 782 Williams, C. A., Collatz, G. J., Masek, J. G., and Goward, S. N.: Carbon consequences of
783 forest disturbance and recovery across the conterminous United States, *Glob.*
784 *Biogeochem. Cycles*, 26, GB1005, 10.1029/2010GB003947, 2012.
- 785 Wolter, P. T., and White, M. A.: Recent forest cover type transitions and landscape
786 structural changes in northeast Minnesota, USA, *Landscape Ecology*, 17, 133-
787 155, 2002.
- 788 Zaehle, S., Medlyn, B. E., De Kauwe, M., Walker, A. P., Dietze, M. C., Hickler, T., Luo,
789 Y., Wang, Y.-P., El-Masri, B., Thornton, P. E., Jain, A. K., Wang, S., Warlind,
790 D., Weng, E., Parton, W. J., Iversen, C. M., Gallet-Budynek, A., McCarthy, H. R.,
791 Finzi, A. C., Hanson, P. J., Prentice, I. C., Oren, R., and Norby, R. J.: Evaluation
792 of 11 terrestrial carbon–nitrogen cycle models against observations from two
793 temperate Free-Air CO₂ Enrichment studies, *New Phytol.*, 202, 803-822,
794 10.1111/nph.12697, 2014.
- 795 Zhao, M., Xiang, W., Peng, C., and Tian, D.: Simulating age-related changes in carbon
796 storage and allocation in a Chinese fir plantation growing in southern China using
797 the 3-PG model, *Forest Ecol. Manage.*, 257, 1520-1531,
798 10.1016/j.foreco.2008.12.025 2009.

799 **Table 1.** Comparison of the models used in this study.

	Model		
	Biome-BGC	ZELIG	ED
Category	Big-leaf	Gap	Gap hybrid
Timestep	Daily	Monthly	Hourly
Spatial scale	Indeterminate	400 m ² cells (gaps)	Variable
Nitrogen cycle?	Yes	No	No
Soil model	4 pools	1 pool; pseudo bucket-model	8 pools
Phenology	Calculated based on soil temperature	Seasonal heat sum, growing degree days	Calculated based on monthly air temperature
Allocation	Fixed ratios	Fixed ratios	Allometric
Canopy	Two layers, sun and shade	Species-specific	Both PFT-specific (individual) and distributional (site)
GPP	Enzyme kinetic: Farquhar, Ball-Berry	APAR and LUE	Enzyme kinetic: Farquhar, Ball-Berry
Respiration	Q ₁₀ , modified by temperature and moisture	Modified by temperature	Arrhenius, modified by temperature and moisture
Succession	None	Species-specific	PFT-specific
Mortality	Fixed rate	Competition driven,	From size- and age-

stochastic

structure PDEs

800

801

802 **Table 2.** Selected site-specific parameters used by Biome-BGC. Model inputs differ from
 803 observed because of the optimization procedure used (see Methods).

Parameter	Observed value (\pm se)	Model value	Units
Fine root C:N ratio	77	77.0	kg C kg N ⁻¹
Fine root:leaf C allocation	1.18	1.14	Ratio
Fraction of leaf N in Rubisco		0.12	Fraction
Leaf C:N ratio	25 \pm 3.4	25.0	kg C kg N ⁻¹
Maximum stomatal conductance	0.03	0.0065	m s ⁻¹
Nitrogen deposition	0.00085	0.001	kg N m ⁻² yr ⁻¹
Specific leaf area		19.42	m ² kg C ⁻¹
Stem:leaf C allocation	1.16	1.16	Ratio
Whole plant mortality fraction	0.014	0.015	1 yr ⁻¹

804

805 **Table 3.** Species-specific allometric and ecological parameters for the 8 tree species used
 806 in ZELIG, representing species found in the Upper Great Lakes. Species shown include
 807 *Populus grandidentata* (POGR), *Betula papyrifera* (BEPA), *Quercus rubra* (QURU),
 808 *Pinus strobus* (PIST), *Acer saccharum* (ACSA), *Acer rubrum* (ACRU), *Populus*
 809 *tremuloides* (POTR), and *Fagus grandifolia* (FAGR). All species were assigned a
 810 probability factor of stress mortality of 0.369, probability factor of natural mortality of
 811 2.408, zone of seed influence of 200. Full explanations for all parameters can be found in
 812 the original ZELIG paper (Urban, 1990).

Species	Age	DBH	HT	G	DegD	DegD	L	D	N	RSER	Stock
	max	max	max		min	max					
POGR	150	70	30	42	800	3169	4	5	2	0.82	0.8
PIST	450	150	37	68	800	3183	3	2	3	0.90	0.7
QURU	400	100	30	92	800	4903	2	3	2	0.44	0.7
ACRU	150	100	30	244	800	6986	2	2	1	0.56	0.8
BEPA	140	100	25	160	800	2500	4	3	3	0.33	0.2
FAGR	366	80	30	100	800	5894	2	2	2	0.44	0.5
ACSA	400	150	40.1	89	800	3200	1	2	2	0.30	0.4
POTR	150	75	37	158	889	5556	4	3	2	0.50	0.4

813 Key: Age_{max}, maximum age for the species (yr); DBH_{max}, maximum diameter at breast
 814 height (cm); HT_{max}, maximum height (m); G, growth rate scaling coefficient; DegD_{min},
 815 minimum growing degree-day; DegD_{max}, maximum growing degree-day; Light (L),
 816 Drought (D), Nutrient (N): light/shade tolerance class, maximum drought tolerance class,

817 and soil nutrient tolerance class; RSER, relative seedling establishment rate; Stock,
818 regeneration stocking.

819

820 **Table 4.** Allometric and ecological parameters used in the ED model. The two plant
 821 functional types represent generic cold deciduous hardwood and evergreen needleleaf
 822 trees, respectively.

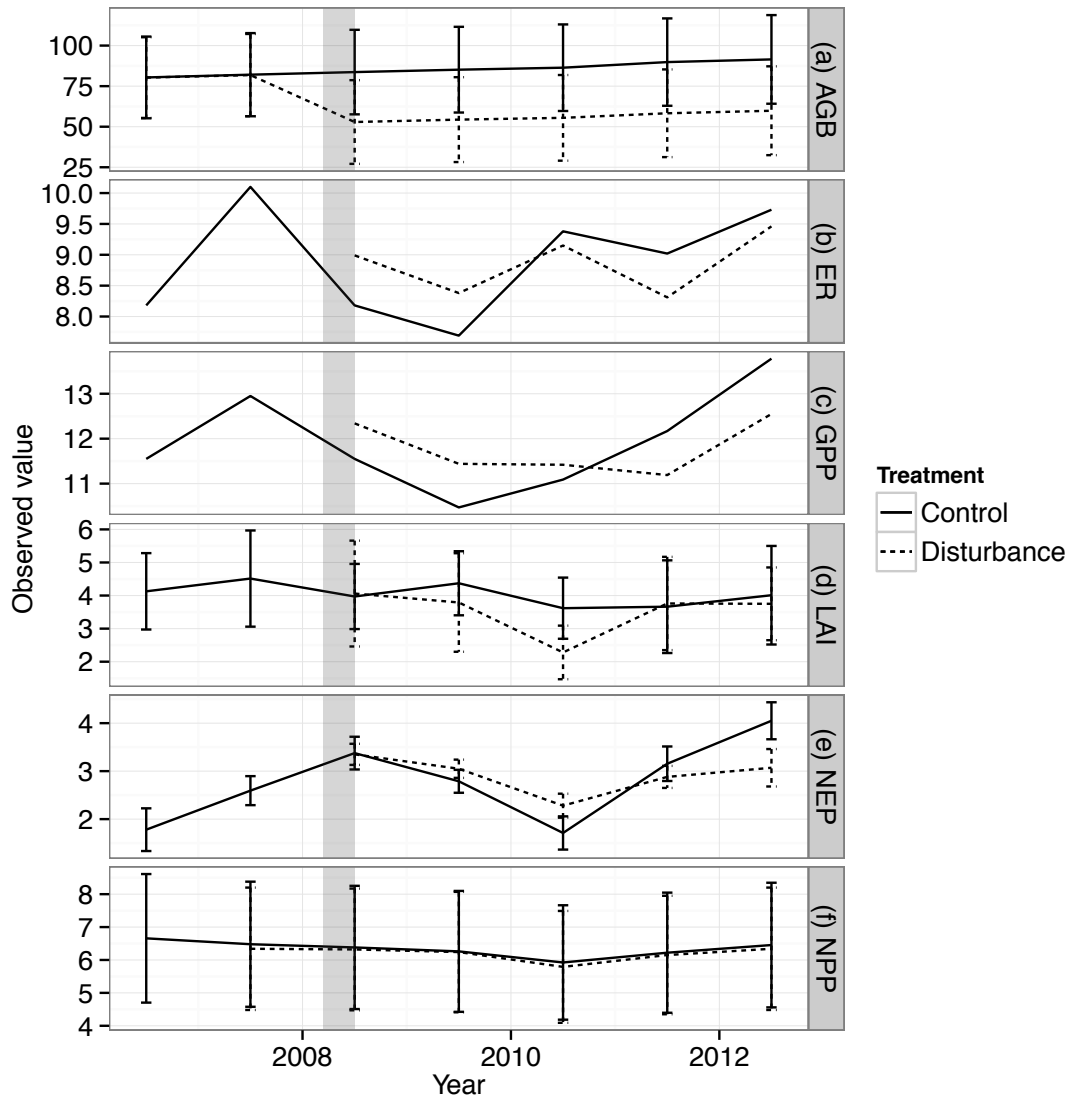
Parameter	Cold Deciduous	Evergreen	Units
V_{\max}	12.5	12.5	$\mu\text{mol m}^{-2} \text{s}^{-1}$
Height computation ¹	$H = 2.34D^{0.64}$	$H=1.04D^{0.94}$	m (H) and cm (D)
Max height	35	35	m
Specific leaf area	18.2	5.5	$\text{m}^2 \text{kg C}^{-1}$
Phenology temperature	10	-	°C
Density-independent mortality	0.014	0.014	1 yr^{-1}

823 ¹Height (H, m) is computed based on DBH (D, cm).

824

825 **Figure 1.** Observed data from FASET treatment and control forests. Panels include (a)
826 aboveground biomass (AGB, in Mg C ha^{-1}), (b) ecosystem respiration (ER, Mg C ha^{-1}),
827 (c) GPP (Mg C ha^{-1}), (d) leaf area index (LAI, unitless), (e) net ecosystem production
828 (NEP, Mg C ha^{-1}), and (f) net primary production (NPP, Mg C ha^{-1}). Vertical shaded area
829 shows approximate time of the girdling treatment described in the text. Error bars
830 indicate ± 1 SD based on eight measurement plots (Gough et al., 2013). Control and
831 treatment sites had near-identical data in 2006 and 2007, and thus the latter (dashed) line
832 is not visible in panels (a), (d), and (f) in those years.

Modeling subtle disturbances in aging forests

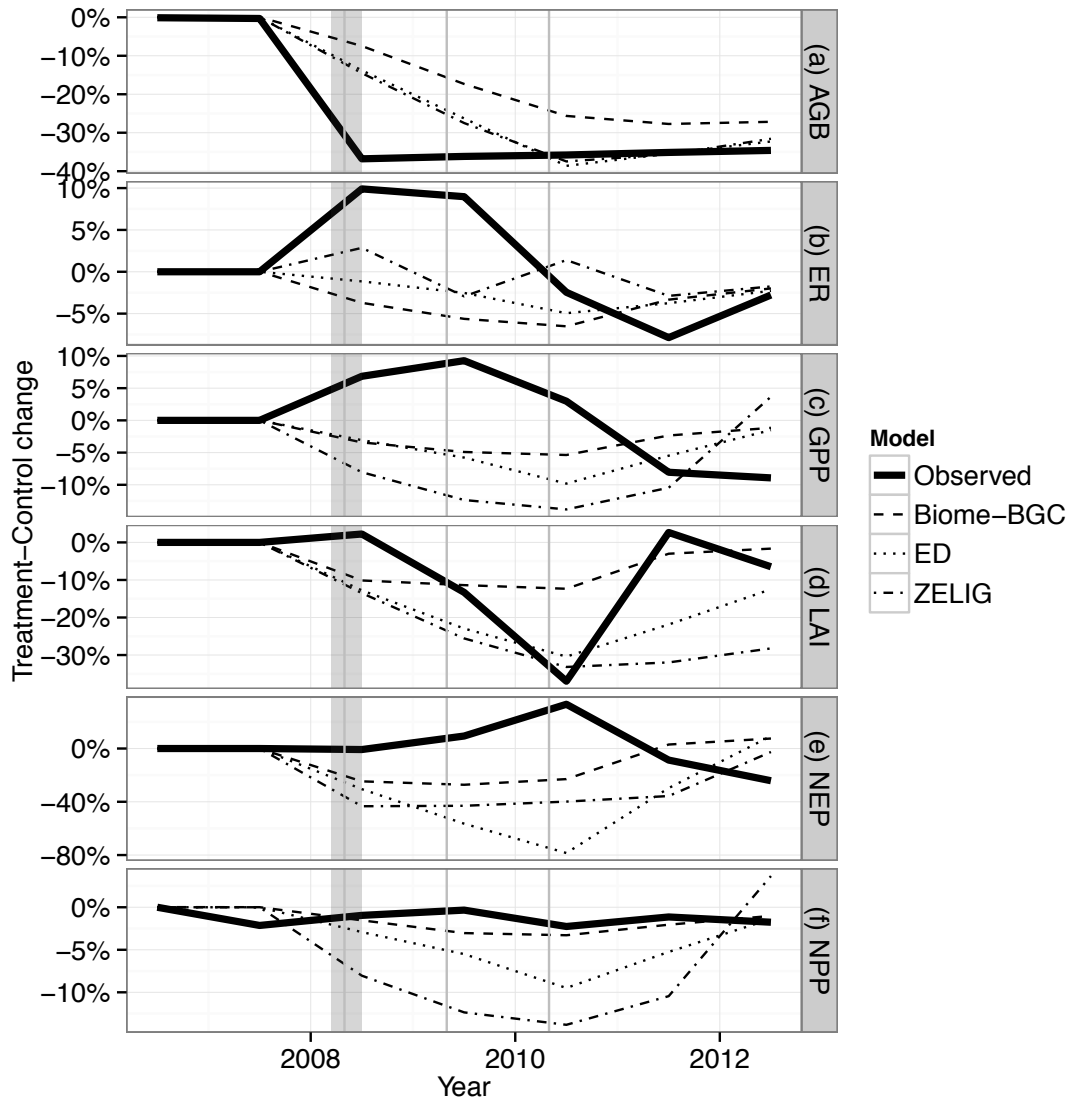


833

834

835 **Figure 2.** Model performance in replicating the FASET experiment. Panels include (a)
836 aboveground biomass (AGB, in Mg C ha^{-1}), (b) ecosystem respiration (ER, Mg C ha^{-1}),
837 (c) GPP (Mg C ha^{-1}), (d) leaf area index (LAI, unitless), (e) net ecosystem production
838 (NEP, Mg C ha^{-1}), and (f) net primary production (NPP, Mg C ha^{-1}), all expressed on a
839 common normalized scale (relative change between treatment and control). Vertical
840 shaded area shows approximate time of the girdling treatment described in the text.
841 Vertical lines show May 1 forest harvests imposed in the Biome-BGC, ED, and ZELIG
842 models.

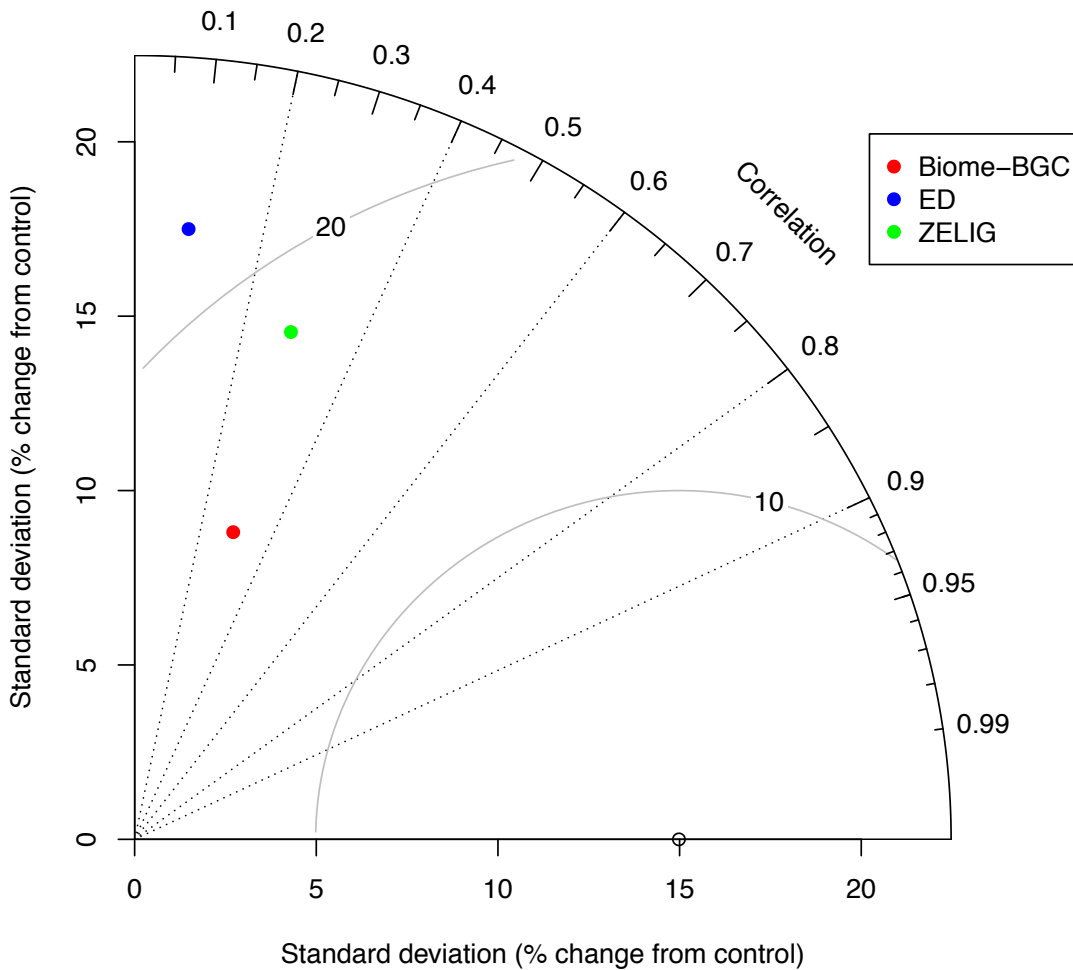
Modeling subtle disturbances in aging forests



843

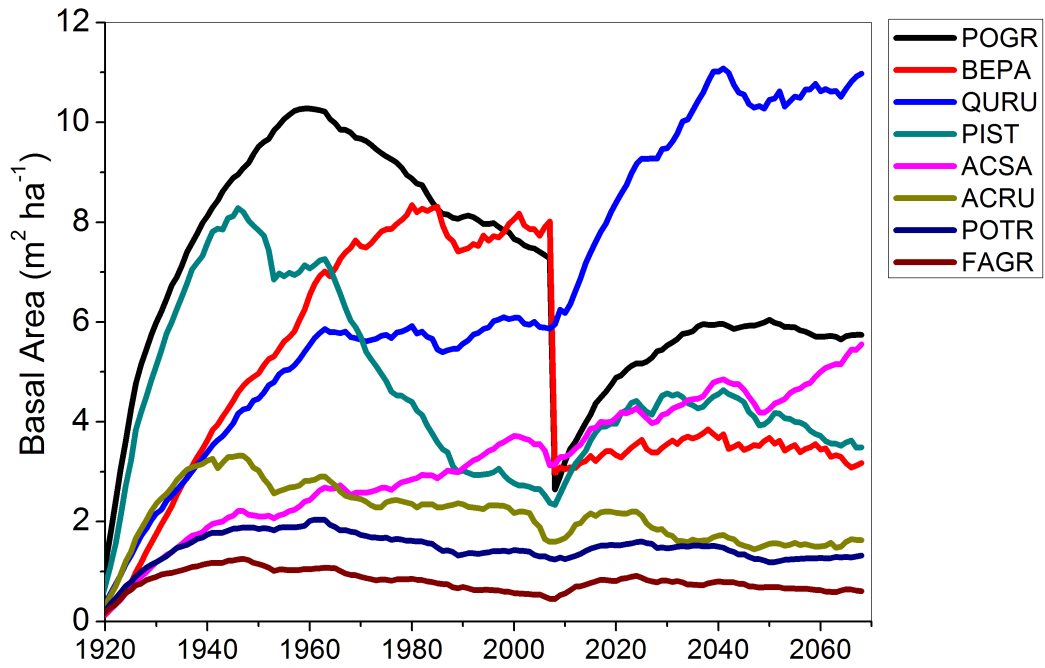
844

845 **Figure 3.** Taylor diagram (Taylor, 2001) summarizing model skill at predicting all
 846 (AGB, ER, GPP, LAI, NEP, NPP; cf. **Figure 1**) observed data, normalized relative to the
 847 control forest. The standard deviation of the simulated data (colored by model) is gauged
 848 by the radial distance from the origin, and can be compared to the observed data (circle
 849 on horizontal axis); model correlation to observations is found by azimuthal position; and
 850 the curves contours show root mean square error (%).



851

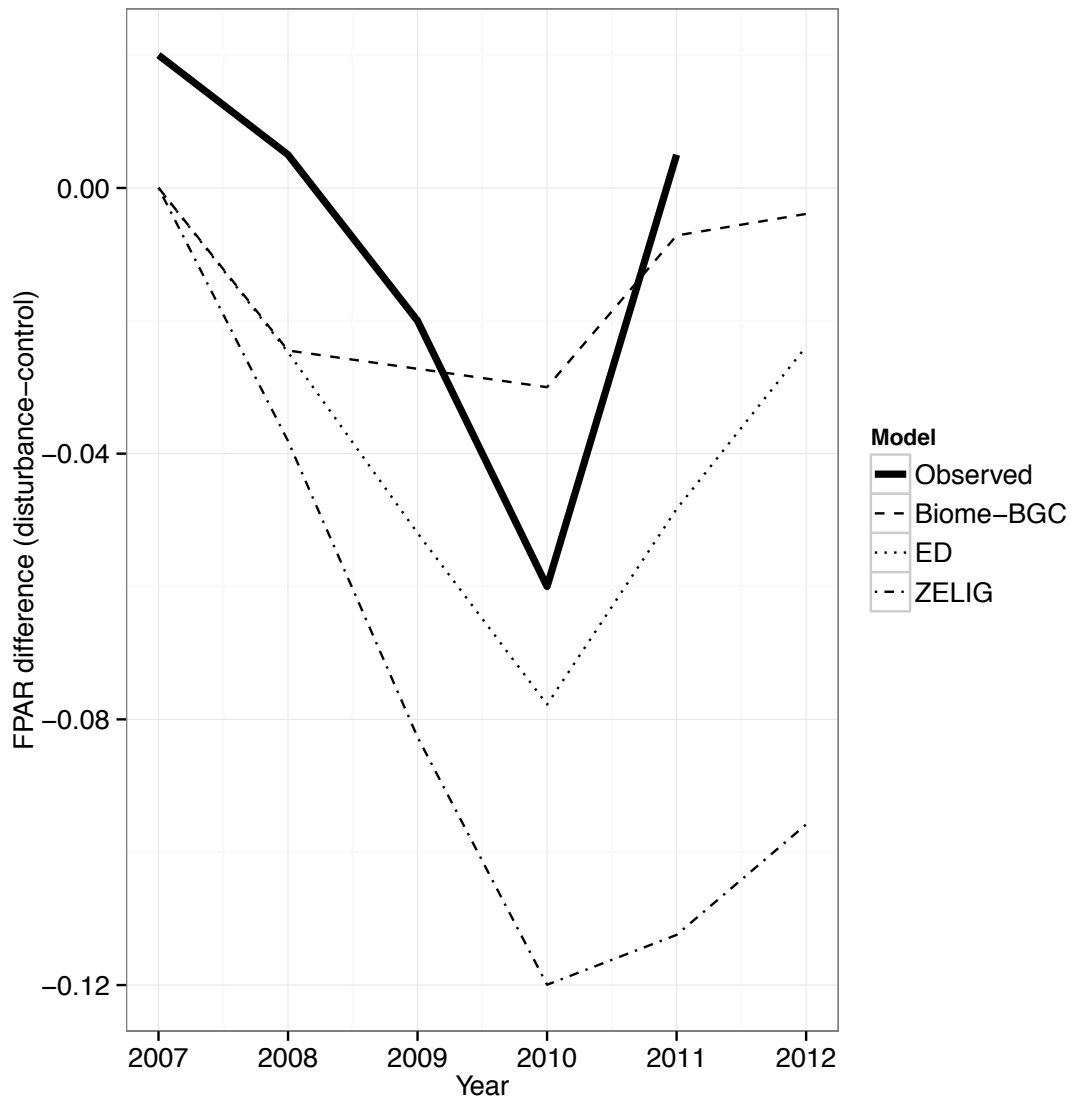
852 **Figure 4.** Species-specific basal area trajectories simulated by ZELIG, before and after
853 the 2008-2010 tree removals mimicking the FASET experiment. Species codes are as in
854 **Table 1.**



855

856

857 **Figure 5.** Effect of disturbance effect on fraction of photosynthetically active radiation
 858 absorbed by the canopy (FPAR). Observed line is based on data from Figure 4 in Gough
 859 et al. (2013). Model lines show implied (i.e. theoretical, based on Beer’s law) FPAR
 860 based on the observed and modeled leaf area index values and a common extinction
 861 coefficient of $k=-0.45$, the model mean.



862

863